Structure and Electron Counting in Ternary Transition Metal Hydrides

Timothy K. Firman and Clark R. Landis*

Contribution from the Department of Chemistry, University of Wisconsin—Madison, 1101 University Avenue, Madison, Wisconsin 53706

Received August 3, 1998. Revised Manuscript Received October 9, 1998

Abstract: A large number of ternary hydrides of transition metals and alkali or alkaline earth metals have been synthesized and structurally characterized in the last twenty years. These compounds exhibit a puzzling variety of compositions, transition metal coordination numbers, transition metal coordination geometries, and distribution of hydrides within and outside of the transition metal coordination sphere. Valence Bond (VB) concepts form a theoretical framework for understanding, at least partially, some of the dominant trends observed among various transition metal hydride structures. Extrapolation of these concepts suggests that synthesis of ternary metal hydrides with formal electron counts at the transition metal exceeding 18 electrons may be feasible.

Introduction

Simple models of chemical bonding are verified or rejected by their compatibility with both empirical and theoretical results. Recently, a large number of ternary metal hydrides[1] having the general formula $A_xM_yH_z$, for which A is an alkali or alkaline earth and M is a transition metal, have been synthesized and characterized by diffraction methods.[2,3] Many of these new compounds have come via high-temperature, high-pressure synthetic routes.

Ternary metal hydrides exhibit a perplexing range of compositions, topologies, and coordination geometries (Table 1). Perhaps the most perplexing feature of these complexes is the occurrence of both transition metal-coordinated hydrides and alkali- or alkaline earth-coordinated hydrides, which we will refer to as interstitial hydrides. The factors controlling the distribution of hydrides between transition metal coordinated and interstitial positions and the overall composition are not well understood.[4] Also perplexing is the variety of coordination numbers (from 2 to 9) and geometries found at the transition metal centers.

Herein, we extend our previously reported Valence Bond (VB) model[5,6] to propose rules for electron counting and structure rationalization of the ternary metal hydrides. We address two primary questions: What controls the number of hydrides coordinated to the metal? How can the geometries of the transition metal centers be understood? Our goal is to address these questions using a simplistic localized bonding model. As a result, many subtle features impacting these structures, such as lattice effects and long-range electron delocalization, will be overlooked. We begin our discussion with a brief review of VB concepts as they apply to transition metal complexes. This is followed by a detailed description of ternary metal hydrides having formal 14, 16, and 18 electron counts. We conclude with some remarks concerning the 18 electron (or EAN) rule and the search for stable metal complexes that exceed the 18 electron count.

Results and Discussion

Valence Bond Concepts. Previously we have shown that the geometries of transition metal hydride and alkyl complexes can be considered the outcome of hybridization of the valence s and d metal atomic orbitals to give sd^n metal hybrid orbitals.[5,6,49,50] The shapes of these metal hybrid orbitals control the

(1) Throughout, we refer to the topic of this paper as ternary metal hydrides even though most of the experimental characterizations are for the ternary metal deuterides.

(2) Bau, R. *Inorg. Chim. Acta* **1997**, *259*, 27−50.
(3) Bronger, W. *J. Alloys Compd.* **1995**, *229*, 1−9.
(4) Bonhomme, F.; Stetson, N. T.; Yvon, K.; Fischer, P.; Hewat, A. W. *J. Alloys Compd.* **1993**, *200*, 65−68.
(5) Landis, C. R.; Firman, T. K.; Root, D. M.; Cleveland, T. *J. Am. Chem. Soc.* **1998**, *120*, 1842−1854.
(6) Landis, C. R.; Cleveland, T.; Firman, T. K. *J. Am. Chem. Soc.* **1998**, *120*, 2641−2649.
(7) Bronger, W.; à Brassard, L. *Z. Anorg. Allg. Chem.* **1996**, *622*, 462−464.
(8) Kadir, K.; Noréus, D. *Z. Phys. Chem.* **1989**, *163*, 231−232.
(9) Noréus, D.; Törnroos, A.; Börje, A.; Szabó, T.; Bronger, W.; Spittank, H.; Auffermann, G.; Müller, P. *J. Less-Common Met.* **1988**, *139*, 233−239.
(10) Bronger, W.; Jansen, K.; Müller, P. *J. Less-Common Met.* **1990**, *161*, 299−302.
(11) Bronger, W.; Auffermann, G. *J. Less-Common Met.* **1990**, *158*, 163−167.
(12) Bonhomme, F.; Yvon, K. *J. Alloys Compd.* **1992**, *186*, 309−314.
(13) Bonhomme, F.; Yvon, K.; Triscone, G.; Jansen, K.; Auffermann, G.; Müller, P.; Bronger, W.; Fischer, P. *J. Alloys Compd.* **1992**, *178*, 161−166.
(14) Cerny, R.; Bonhomme, F.; Yvon, K.; Fischer, P.; Zolliker, P.; Cox, D. E.; Hewat, A. *J. Alloys Compd.* **1992**, *187*, 233−241.
(15) Bronger, W.; Müller, P.; Schmitz, D.; Spittank, H. *Z. Anorg. Allg. Chem.* **1984**, *516*, 35−41.
(16) Bronger, W.; Auffermann, G.; Müller, P. *J. Less-Common Met.* **1986**, *116*, 9−15.
(17) Bronger, W.; Auffermann, G.; Müller, P. *J. Less-Common Met.* **1988**, *142*, 243−252.
(18) Bronger, W.; Auffermann, G. *J. Alloys Compd.* **1995**, *228*, 119−121.
(19) Bronger, W.; Auffermann, G.; Müller, P. *Z. Anorg. Allg. Chem.* **1988**, *566*, 31−38.
(20) Bronger, W.; Auffermann, G. *J. Alloys Compd.* **1992**, *187*, 81−85.
(21) Bronger, W.; Auffermann, G. *J. Alloys Compd.* **1992**, *179*, 235−240.
(22) Bronger, W.; à Brassard, L. *Angew. Chem., Int. Ed. Engl.* **1995**, *34*, 898−900.
(23) Kadir, K.; Noréus, D. *Z. Phys. Chem.* **1993**, *179*, 237−242.
(24) Bronger, W.; Müller, P.; Kowalczyk, J.; Auffermann, G. *J. Alloys Compd.* **1991**, *176*, 263−268.
(25) Lundberg, L. B.; Cromer, D. T.; Magee, C. B. *Inorg. Chem.* **1972**, *11*, 400−404.

10.1021/ja982746r CCC: $15.00
Published on Web 11/20/1998

Table 1. Ternary Metal Hydrides, Electron Counts, Resonance Formulations, and Coordination Geometries

compound	electron count	primary resonance structure[a] $aA^{w}\{dH^{-}\}\ [MH_b{}^{x}\ cH^{-}]$	coordination geometry
Li_2PtH_2[7]	14	$2Li^+$ **[**$PtH^-\ H^-$**]**	linear
A_2PdH_2 (A ≡ Li,[8] Na[9])	14	$2Na^+$ **[**$PdH^-\ H^-$**]**	linear
$CaPdH_2$[10]	14	$2Na^+$ **[**$PdH^-\ H^-$**]**	linear
K_3PdH_3[11]	14	$3K^+\{H^-\}$**[**$PdH^-\ H^-$**]**	linear
Mg_3RuH_3[12]	14	$3Mg^+$ **[**$RuH_2{}^{2-}\ H^-$**]**	T-shape
Mg_4IrH_5[4]	14	$4Mg^+\ \{2H^-\}$**[**$IrH_2{}^-\ H^-$**]**	T-shape
Mg_2RuH_4[13]	14	$2Mg^+$ **[**$RuH_3{}^-\ H^-$**]**	seesaw
$Mg_{12}Co_4H_{22}$[14]	14	$9Mg^+\ 3$**[**$CoH_3\ H^-$**]**	seesaw
	16	$3Mg^0\{5H^-\}$**[**$CoH_3\ 2H^-$**]**	square pyramidal (monovacant O_h)
A_2PtH_4 (A ≡ Na,[15] K,[16] Rb,[17] Cs[17])	16	$2A^+$ **[**$PtH_2\ 2H^-$**]**	square planar
Na_2PdH_4[18]	16	$2Na^+$ **[**$PdH_2\ 2H^-$**]**	square planar
A_3PtH_5[19] (A ≡ K, Rb, Cs)	16	$2A^+\ \{H^-\}$**[**$PtH_2\ 2H^-$**]**	square planar
A_3PdH_5 (A ≡ K,[20] Rb,[21] Cs[20])	16	$2A^+\ \{H^-\}$**[**$PdH_2\ 2H^-$**]**	square planar
$Li_5Pt_2H_9$[22]	16	$5Li^+\ \{H^-\}\ 2$**[**$PtH_2\ 2H^-$**]**	square planar
A_2PtH_6[23] (A ≡ Sr, Ba)	16	$2A^{2+}\ \{2H^-\}$**[**$PtH_2\ 2H^-$**]**	square planar
Li_3RhH_4[24]	16	$3Li^+$ **[**$RhH_2{}^-\ 2H^-$**]**	square planar
Li_4RhH_5[25]	16	$4Li^+\ \{H^-\}$**[**$RhH_2{}^-\ 2H^-$**]**	square planar
A_2IrH_5 (A ≡ Ca,[26] Sr[26,27])	16	$2A^+$ **[**$IrH_3\ 2H^-$**]**	square pyramidal (monovacant O_h)
A_2RhH_5 (A ≡ Ca,[26] Sr[26,28])	16	$2A^+$ **[**$RhH_3\ 2H^-$**]**	square pyramidal (monovacant O_h)
$Ca_4Mg_4Co_3H_{19}$[29]	16	$4Mg^+\ 2Ca^{2+}\ 2Ca^+\ \{4H^-\}$ 3**[**$CoH_3\ 2H^-$**]**	square pyramidal (monovacant O_h)
Mg_2CoH_5[30]	16	$2Mg^+$ **[**$CoH_3\ 2H^-$**]**	square pyramidal (monovacant O_h)
Mg_3RuH_6[31]	16	$1Mg^{2+}\ 2Mg^+\ \{H^-\}$**[**$RuH_3{}^-\ 2H^-$**]**	square pyramidal (monovacant O_h)
A_2FeH_6 (A ≡ Mg,[32] Ca,[33] Sr,[33] Eu[33])	18	$2A^{2+}$ **[**$FeH_3{}^-\ 3H^-$**]**	octahedral
A_2RuH_6 (A ≡ Mg,[33,34] Ca,[26] Sr,[26] Ba[34])	18	$2A^{2+}$ **[**$RuH_3{}^-\ 3H^-$**]**	octahedral
A_2OsH_6 (A ≡ Mg,[35] Ca,[33,34] Sr,[34] Ba[34])	18	$2A^{2+}$ **[**$OsH_3{}^-\ 3H^-$**]**	octahedral
A_3RhH_6 (A ≡ Li,[36] Na[37])	18	$3A^+$ **[**$RhH_3\ 3H^-$**]**	octahedral
K_3ReH_6[38]	16	$3K^+$ **[**$ReH_3\ 3H^-$**]**	octahedral
A_4RuH_6[39] (A ≡ Li, Na)	18	$4A^+$**[**$RuH_3{}^-\ 3H^-$**]**	octahedral
Li_4OsH_6[39]	18	$4Li^+$**[**$OsH_3{}^-\ 3H^-$**]**	octahedral
A_3IrH_6[37] (A ≡ Li, Na)	18	$3A^+$ **[**$IrH_3\ 3H^-$**]**	octahedral
A_2PtH_6 (A ≡ Na,[40] K,[41] Rb,[42] Cs[42])	18	$2A^+$ **[**$PtH_3{}^+\ 3H^-$**]**	octahedral
$LiMg_2RuH_7$[43]	18	$Li^+\ 2Mg^{2+}\ \{H^-\}$**[**$RuH_3{}^-\ 3H^-$**]**	octahedral
Mg_3ReH_7[44]	18	$3Mg^{2+}\ \{H^-\}$**[**$ReH_3{}^{2-}\ 3H^-$**]**	octahedral
$BaMg_2MH_8$ (M ≡ Fe,[45] Ru,[46] Os[46])	18	$Ba^{2+}\ 2Mg^{2+}\ \{2H^-\}$**[**$MH_3{}^-\ 3H^-$**]**	octahedral
$Ba_3Ir_2H_{12}$[47]	18	$3Ba^{2+}\ 2$**[**$IrH_3\ 3H^-$**]**	octahedral
$LiMg_4Os_2H_{13}$[48]	18	$Li^+\ 4Mg^{2+}\ \{H^-\}\ 2$**[**$OsH_3{}^-\ 3H^-$**]**	octahedral

[a] In the resonance formula, *a* is the number and *w* is the formal charge on the alkaline earth or alkali metal, {} indicate interstitial hydrides, *d* is the number of interstitial hydrides, **[]** indicate the metal coordination complex, *b* is the number of transition metal-coordinated hydrogens in the 12 electron fragment, *x* is the formal charge on the metal, and *c* is the number of $3c-4e^-$ bonds at the transition metal.

shapes of the transition metal complexes (in the absence of steric effects). The idealized arrangements of metal hybrid orbitals are summarized in Figure 1. As Figure 1 illustrates, the lobes of sd^1 hybrids point to the corners of a square, those of sd^2 hybrids point to the vertices of an octahedron, those of sd^3 hybrids point along the body diagonals of a cube, and those of sd^5 hybrids are directed to the vertices of an icosahedron. The hybridization of M−H bonds is determined by the total number of electrons in the metal complex and the number of lone pairs and M−H bonds. For simplicity we will consider only diamagnetic complexes in this summary. If the total number of electrons is 12 or less, the hybridization of each M−H bond is sd^{n-1},

(26) Moyer, R. O. J.; Stanitski, C.; Tanaka, J.; Kay, M. I.; Kleinberg, R. *J. Solid State Chem.* **1971**, *3*, 541−549.
(27) Zhuang, J.; Hastings, J. M.; Corliss, L. M.; Bau, R.; Wei, C.-Y.; Moyer, R. O. J. *J. Solid State Chem.* **1981**, *40*, 352−360.
(28) Bronger, W.; Beissmann, R.; Ridder, G. *J. Alloys Compd.* **1994**, *203*, 91−96.
(29) Huang, B.; Yvon, K.; Fischer, P. *J. Alloys Compd.* **1995**, *227*, 116−120.
(30) Zolliker, P.; Yvon, K.; Fischer, P.; Schefer, J. *Inorg. Chem.* **1985**, *24*, 4177−4180.
(31) Bronger, W.; Jansen, K.; Auffermann, G. *J. Alloys Compd.* **1993**, *199*, 47−51.
(32) Didisheim, J.-J.; Zolliker, P.; Yvon, K.; Fischer, P.; Schefer, J.; Gubelmann, M.; Williams, A. F. *Inorg. Chem.* **1984**, *23*, 1953−1957.
(33) Huang, B.; Bonhomme, F.; Selvam, P.; Yvon, K.; Fisher, P. *J. Less-Common Met.* **1991**, *171*, 301−311.
(34) Kritikos, M.; Noréus, D. *J. Solid State Chem.* **1991**, *93*, 256.
(35) Kritikos, M.; Noréus, D.; Bogdanovic, B.; Wilczok, U. *J. Less-Common Met.* **1990**, *161*, 337−340.
(36) Bronger, W.; Gehlen, M.; Auffermann, G. *Z. Anorg. Allg. Chem.* **1994**, *620*, 1983−1985.
(37) Bronger, W.; Gehlen, M.; Auffermann, G. *J. Alloys Compd.* **1991**, *176*, 255−262.
(38) Bronger, W.; Auffermann, G.; Schilder, H. *Z. Anorg. Allg. Chem.* **1998**, *624*, 497−500.
(39) Kritikos, M.; Noréus, D.; Andresen, A. F.; Fischer, P. *J. Solid State Chem.* **1991**, *92*, 514−519.
(40) Bronger, W.; Auffermann, G. *J. Alloys Compd.* **1995**, *219*, 45−47.
(41) Bronger, W.; Auffermann, G. *Angew. Chem., Int. Ed. Engl.* **1994**, *33*, 1112−1114.
(42) Bronger, W.; Auffermann, G. *Z. Anorg. Allg. Chem.* **1995**, *621*, 1318−1321.
(43) Huang, B.; Yvon, K.; Fischer, P. *J. Alloys Compd.* **1994**, *210*, 243−246.
(44) Huang, B.; Yvon, K.; Fischer, P. *J. Alloys Compd.* **1993**, *197*, 97−99.
(45) Huang, B.; Yvon, K.; Fischer, P. *J. Alloys Compd.* **1995**, *227*, 121−124.
(46) Huang, B.; Gingl, F.; Fauth, F.; Hewat, A.; Yvon, K. *J. Alloys Compd.* **1997**, *248*, 13−17.
(47) Kadir, K.; Noréus, D. *J. Alloys Compd.* **1994**, *209*, 213-215.
(48) Huang, B.; Fischer, P.; Yvon, K. *J. Alloys Compd.* **1996**, *245*, L24-L27.
(49) Landis, C. R.; Cleveland, T.; Firman, T. K. *J. Am. Chem. Soc.* **1995**, *117*, 1859−1860.
(50) Landis, C. R.; Cleveland, T.; Firman, T. K. *Science* **1996**, *272*, 179.

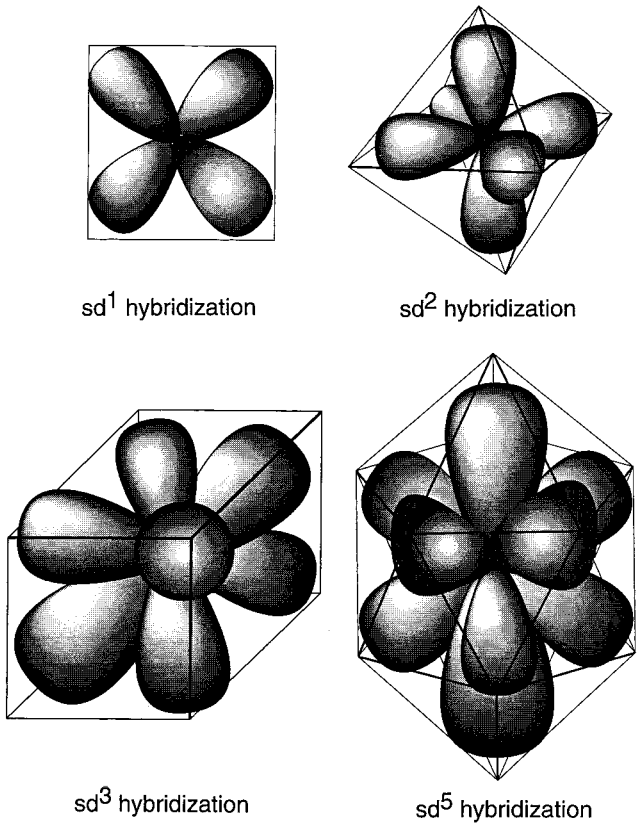

Figure 1. Orientations of sd^n hybrid orbitals and their corresponding polyhedral coordination geometries.

where *n* is the number of coordinated hydrides. The remaining electrons occupy the other pure d atomic metal orbitals to make metal lone pairs. In our model,[5,6,49,51] lone pairs do not exert steric effects that significantly impact the geometry beyond making those metal d orbitals unavailable for bonding.

Transition metal hydrides with more than 12 electrons are considered hypervalent in our VB scheme. In general, hypervalency gives rise to a number of delocalized 3 center-4 electron (3c-4e$^-$) bonding interactions, each involving the overlap of a central atom "sd^n hybrid atomic orbital" with the two 1s H atomic orbitals. In VB theory, these units are described as a resonance between two ionic configurations. For example, the VB description of the 3c-4e$^-$ bond in XeF_2 is illustrated below:

XeF_2: $F\text{-}Xe^{+}\ F^{-} \longleftrightarrow {}^{-}F\ Xe^{+}\text{—}F$ ≈ 3 center-4 electron bond

For transition metal hydrides, every pair of electrons greater than 12 requires one 3c-4e$^-$ bonding interaction. For example, the 16 electron dianion, $[PtH_4]^{2-}$, has two 3c-4e$^-$ bonds involving sd^1 metal hybridization (this is readily derived from any one of the resonance configurations shown below). Accordingly, the Pt coordination geometry is square planar (see sd^1 hybrid orbitals in Figure 1). We use the following notation to describe the bonding in the tetrahydridoplatinate dianion: **[**PtH_2 $2H^-$**]**. The bold brackets **[]** indicate the transition metal coordination sphere; within these brackets there is one 3c-4e$^-$ interaction for every hydrogen that is separated from the transition metal symbol by white space.

(51) Root, D. M.; Landis, C. R.; Cleveland, T. *J. Am. Chem. Soc.* **1993**, *115*, 4201−4209.

PtH_4^{2-}: $H\text{—}Pt(H)\text{—}H^- \longleftrightarrow H^-\text{—}Pt(H)\text{—}H$ ≈ two 3 center-4 electron bonds
and 4 lone pairs *and 4 lone pairs*

Previous Theoretical Models of Ternary Metal Hydrides. The structures and compostions of ternary metal hydrides challenge most conventional theoretical models. Noréus[34] has attributed the ability of hydride ligands to stabilize both low- and high-valent transition metals to the large polarizability of the M−H bond, which permits the hydrogen to distribute electron density away from the central atom through its ability to adopt a large radius. Application of this reasoning to the VB concepts discussed above rationalizes why there would be substantial resonance stabilization of the 3c-4e$^-$ bonds involving transition metals with hydride ligands.

Most commonly, the compositions of transition metal hydrides have been rationalized by the 16 and 18 electron rules.[32] However, it has been recognized that compounds such as Na_2PdH_2 do not obey these prescriptions. Furthermore, the formulation of compounds such as Mg_3RuH_3 as either 17 electron monomers or 18 electron dimers[12] of RuH_3^{6-} requires an unreasonably large formal charge of −3 on the Ru atom. Miller and co-workers[52] have provided insightful analysis of the electronic structures of ternary hydrides of Group VIII metals as computed by extended Hückel computations. On the basis of these computations, Miller and co-workers attributed the unusual seesaw geometry of the RuH_4 fragment in Mg_2RuH_4 to a combination of zeroth-order ligand field effects, the low oxidation state of the metal, and both Ru−Ru and Ru−Mg bonding interactions. The same authors interpreted the T-shape coordination geometry of the RuH_3 fragment as the consequence of strong Mg−Ru interactions, emphasizing that Mg atoms do not act as simple dipositive cations and that Ru−Ru bonding interactions are minimal.

A number of researchers[53] have employed computational methods and qualitative MO theory to understand the conductivity properties of metal hydrides, a topic that lies outside the focus of this article.

Fourteen Electron Metal Complexes. The simplest ternary metal hydrides currently characterized are the linear hydrides, Li_2PtH_2,[7] Na_2PdH_2,[9] and $CaPdH_2$.[10] In the VB model of transition metal hydride complexes only the s and d orbitals of the metal are used in bonding, which implies that only 12 electrons can be centered on a metal in any single resonance structure. Let us assume complete valence electron transfer from each alkali or alkaline earth metal to the metal hydride complex. The result is that the $[PdH_2]^{2-}$ unit would have a 14e$^-$ count and formally would be hypervalent.[5] In the VB model, the bonding in $[PdH_2]^{2-}$ is described as a resonance between two Lewis structures, each having a 12 electron $[Pd\text{—}H]^-$ core fragment and a hydride anion. In other words, there is one 3c-4e$^-$ bond.

PdH_2^{2-}: $H\text{—}Pd^-\ H^- \longleftrightarrow H^-\ Pd\text{—}H$ ≈ one 3 center-4 electron bond
and 5 lone pairs *and 5 lone pairs*

The hybridization of the $H\text{—}Pd^-\ H^-$ resonance structure is sd^1 and the formal charge on Pd is −1. Maximum resonance occurs at linear H−Pd−H arrangements, leading to a linear coordination geometry.

(52) Miller, G. J.; Deng, H.; Hoffmann, R. *Inorg. Chem.* **1994**, *33*, 1330−1339.

(53) Kasowski, R. V.; Noréus, D.; Wang, L.; Whangbo, M.-H. *Inorg. Chem.* **1992**, *31*, 4737−4739.

A closely related hydride complex is K_3PdH_3.[11] Interestingly, from diffraction experiments the solid-state structure of K_3PdH_3 has just two hydrides coordinated to the Pd. Thus, rather than adopting a 16 electron $[PdH_3]^{3-}$ coordination with 4 center-6 electron bonding (or resonance among H−Pd$^-$ 2H$^-$ configurations), one hydride is interstitial and octahedrally coordinated by the K^+ ions. Thus, the metal complex is a hypervalent 14 electron species with one 3c-4e$^-$ bond. The coordination geometry of the resulting localized $[PdH_2]^{2-}$ anion is linear as in K_2PdH_2.

We use the following notation to describe the K_3PdH_3 compound: $3K^+$ $\{H^-\}$**[**PdH^- H^-**]**. The bold brackets **[]** define the coordination geometry, charge, and number of 3c-4e$^-$ bonds of the transition metal coordination complex as described above. Hydrides surrounded by curly brackets {} are located in interstitial sites. The charges indicate how we have counted electrons in each of the fragments of the compound. Thus, the solid-state structure of K_3PdH_3 consists of $\{H^-\}$**[**PdH^- H^-**]** fragments which are charged balanced by potassium cations.

As will be shown, this pattern is common for the solid-state structures of ternary metal hydrides and illustrates a general rule: *Hypervalent metal hydrides with delocalizations greater than 3c-4e$^-$ bonding (such as 4 center-6 electron motifs) tend to lose hydrides to the lattice so that 3c-4e$^-$ bonding is maintained*. We will demonstrate a second rule, which essentially is a restatement of Pauling's electroneutrality rule, that also appears to be general: *Metal hydrides with formal metal charges other than −1, 0, and +1 are disfavored.*

Sixteen or Fourteen Electron Metal Complexes? Partial Charge Transfer. Illustrations of the reluctance of ternary metal hydrides to engage in higher level delocalizations are found in the solid-state compositions Li_4RhH_5,[25] A_3PdH_5,[20] and A_3PtH_5.[19] (A ≡ K, Rb, or Cs); each has four hydrides complexed to the transition metal and one interstitial hydride (e.g., $4Li^+$ $\{H^-\}$**[**RhH_2 $2H^-$**]**). Thus, in the solid state these coordination complexes consist of 16 electron $[RhH_4]^{3-}$, $[PdH_4]^{2-}$, and $[PtH_4]^{2-}$ units. According to the VB model, these complexes are built from two 3c-4e$^-$ bonding units with sd^1 bond hybridization. A square planar coordination geometry is expected and indeed is observed for the related solid-state compositions A_2PtH_4 (A ≡ Na, K, Rb, or Cs)[17] and Na_2PdH_4.[18] Similarly, DFT ab initio computations on the isolated $[RhH_4]^{3-}$, $[PdH_4]^{2-}$, and $[PtH_4]^{2-}$ ions yield square planar energy minima.

A sharp contrast to these square planar, 16 electron ions is provided by the superficially isoelectronic Mg_2RuH_4,[13] which exhibits a "seesaw", or cis-divacant octahedral, geometry. This structure, as noted in the orginal report, is "unusual among four-coordinated transition metal complexes".[13] In a subsequent review, Brönger[3] speculated that "This hitherto unkown coordination geometry for a transition metal ion with a d^8 configuration is evidently stabilized by the existence of metal−metal interactions between the ruthenium atoms in the direction of the missing cis-ligands." However, the Ru−Ru separation of 3.24 Å far exceeds the 2.65−3.0 Å range of crystallographically characterized Ru−Ru single bonds. Clearly, the discontinuity in molecular shapes for nominally isoelectronic transition metal complexes, such as Mg_2RuH_4 and Na_2PtH_4, requires careful attention. Let us focus on electron counting in Mg_2RuH_4: Does each of the Mg contribute one or two electrons to the transition metal and hydrogen?

The solid-state structure of Mg_2RuH_4,[13] having a seesaw geometry at Ru with H−Ru−H angles of 84.2°, 93.6°, and 170.3°, is not consistent with divalent magnesium atoms. If each Mg were assumed to transfer two electrons, then 16 electron $[RuH_4]^{4-}$ units, each with a formal −2 charge on Ru, would result. Consequently, a square planar coordination geometry would be expected, as is observed for Na_2PdH_4. However, *transfer of one electron per Mg* generates a 14 electron $[RuH_4]^{2-}$ unit, in which there is one 3c-4e$^-$ bond and two normal 2 center-2 electron bonds (i.e., the resonance structures have the form $[RuH_3^-$ $H^-]$. The three sd^2 bonding orbitals of the $[RuH_4]^{2-}$ complex yield 90° H−Ru−H angles; inclusion of one linear 3c-4e$^-$ bonding interaction completes the seesaw shape (see Figure 1 and Table 1).

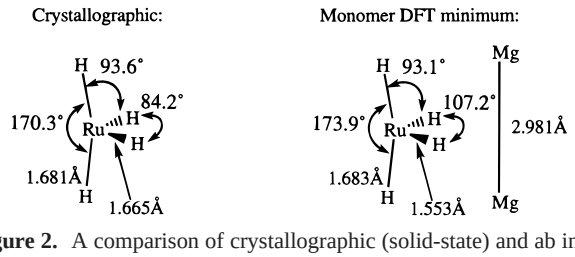

Figure 2. A comparison of crystallographic (solid-state) and ab initio (gas phase) structures of Mg_2RuH_4.

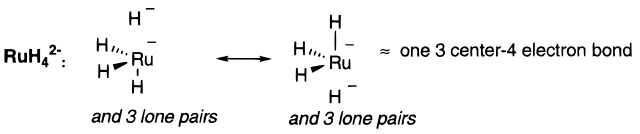

Thus, a VB perspective provides an understanding of this uncommon structure.

In support of our electron counting scheme, the solid-state structure of Mg_2RuH_4 shows that the Mg^+ cations form an extended covalent Mg bonding network with Mg−Mg close contacts of 2.930 and 3.076 Å. For comparison, M_2^{2+} [54] dimers have been postulated in liquid MX_2−M systems (M is alkaline earth, X is halide) and DFT computations on $[Mg_2]^{2+}$ yield a 2.928 Å Mg−Mg distance and a covalent Mg−Mg bond as confirmed by natural bond order (NBO)[55] analysis. In contrast, the Mg_2^{3+} dimer is unbound and the neutral Mg_2 dimer has a weak bond that is 3.5 Å long. Thus, the Mg−Mg separations in the solid-state structure of Mg_2RuH_4 support an electron counting scheme that places one valence electron with each Mg.

DFT computations for the gas-phase Mg_2RuH_4 molecule optimize to the structure shown in Figure 2. Clearly, the geometry about the Ru is the seesaw geometry seen in the experimental solid-state structure of Mg_2RuH_4. NBO analysis of the gas-phase electron density yields a Mg−Mg single bond and a natural charge of +0.83 per Mg; both features support the formation of a covalent Mg−Mg bonding network in the solid-state structure of Mg_2RuH_4. Further support for the prediction of a seesaw geometry for 14 electron, four-coordinate metal hydrides comes from our previous DFT computations[5] on the gas-phase $[RhH_4]^-$ anion, which is isoelectronic with $[RuH_4]^{2-}$ and minimizes to a seesaw geometry.

Our analysis does not preclude significant Mg−Ru and H−Mg interactions in the solid-state structure of Mg_2RuH_4. Indeed, NBO analysis of gas-phase Mg_2RuH_4 indicates significant Ru−Mg delocalization of electron density, and the crystallographic distances for solid-state Mg_2RuH_4 are sufficiently short to support Mg−H and Mg−Ru bonding. Nonetheless, the discussion provided above does suggest that our bonding description captures the dominant contributing resonance structure.

(54) Dworkin, A. S.; Bronstein, H. R.; Bredig, M. A. *J. Phys. Chem.* **1966**, *70*, 2384−2388.

(55) Glendening, E. D.; Badenhoop, J. K.; Reed, A. E.; Carpenter, J. E.; Weinhold, F.; University of Wisconsin: Madison, WI, 1994.

Our description of Mg_2RuH_4 differs from that offered by Miller and co-workers, primarily in the assumption of electron count at the transition metal. Miller and co-workers assume an electron density distribution corresponding to $[RuH_4]^{4-}$. From this starting point, Miller and co-workers rationalize the seesaw geometry of $[RuH_4]^{4-}$, in opposition to the square planar geometry of $[PtH_4]^{2-}$, as a consequence of valence d-orbital ionization energies on charge at the transition metal center. In contrast, our approach emphasizes partial transfer of electrons from Mg to the RuH_4. Partial transfer of valence electrons from alkaline earth metals to transition metal hydrides is presumed to occur whenever transfer of two electrons would yield a complex with higher order delocalizations than 3c-4e$^-$ bonding units or would yield a transition metal with a formal charge other than -1, 0, or $+1$.

An interesting violation of the formal charge rule occurs with the ternary complex, Mg_3RuH_3. The neutron diffraction structure is a T-shape $[RuH_3]^{n-}$ fragment, with H−Ru−H angles of 170.3(3)° and 94.7(2)°; the long 3.31 Å Ru−Ru distance indicates no Ru−Ru bonding. If the magnesium atoms were dications, the Ru hydride coordination complex would be the 17 e$^-$ $[RuH_3]^{6-}$. This is an unreasonable electron count because of the excessively high charge and because, according to the VB model, no resonance structures containing even one covalent Ru−H bond can be drawn. In contrast, if we assume that *each Mg contributes a single electron*, then the bonding in the resulting hypervalent, 14 electron $[RuH_3]^{3-}$ involves sd^1 metal hybridization with one 3c-4e$^-$ interaction. Hence, a T-shape (see Figure 1) is expected due to occupation of three vertices of a square. Similarly, the T-shape is found by DFT computations on the isolated $[RuH_3]^{3-}$ and $[PtH_3]^{1-}$ ions.[5,6] NBO analysis of the DFT electron density of RuH_3^{3-} clearly indicates the presence of a single 3c-4e$^-$ bond. Although the crystallographic structure has similar bond lengths for all Ru−H distances (1.71 Å), in the computed gas-phase structure the pseudoaxial bond lengths are significantly longer than the pseudoequatorial bond length (1.72 Å vs 1.58 Å). We note that the position of the pseudoequatorial ligand in the crystallographic structure is disordered over two sites and is less well-determined.

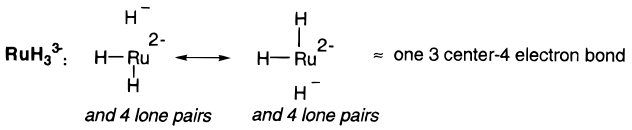

A 14e$^-$ $[RuH_3]^{3-}$ complex implies a $+1$ charge on Mg and a -2 formal charge on Ru. As for Mg_2RuH_4, Mg_3RuH_3 exhibits short Mg−Mg distances, consistent with the Mg−Mg bonding character expected for univalent Mg. We might expect this complex to be unstable with respect to expulsion of a H$^-$, thus lowering the total charge to -1. Mg_3RuH_3 appears to accommodate the high formal charge at the Ru through close Mg−H contacts. Each H has Mg contacts at just over 2 Å (a single Mg−H distance of 2.065 Å for the pseudoaxial H's and two 2.012 Å contacts for the pseudoequatorial H), suggesting significant electron delocalization via Ru−H−Mg bridges. For comparison, MgH_2 exhibits Mg−H bond distances of 1.95 Å. Alternatively, one could view the Ru as exhibiting bonding interactions with the Mg; the shortest Mg−Ru separations are 2.73 Å.

Our analysis of the Mg_3RuH_3 electronic structure shares important features with the analysis of Miller and co-workers. Most importantly, both approaches emphasize that Mg are not well-described as $+2$ cations. Also, both analyses downplay the importance of Ru−Ru bonding and suggest significant Mg−Ru interaction.

Table 2. DFT(B3LYP) Minima for Sr_2RhH_5

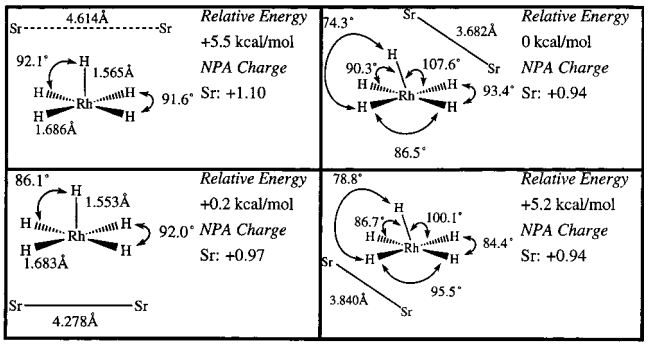

Sixteen or Eighteen Electron Metal Complexes? Partial Charge Transfer. Although ostensibly similar, the ternary hydrides Li_4RhH_5[25] and Sr_2RhH_5[26] exhibit different structures: in the Li compound one hydride is interstitial and four hydrides are coordinated to Rh whereas the Sr compound has all five hydrides coordinated to Rh. Thus, as illustrated below, the topology of Sr_2RhH_5 corresponds to that expected for a 16 electron metal hydride generated by transfer of one electron from each Sr ($2Sr^+$ **[**RhH_3 $2H^-$**]** with two 3c-4e$^-$ bonds and sd^2 hybridization). If the Sr were to contribute two electrons each to generate an 18 electron metal hydride anion and two Sr^{2+} ions, our rules suggest that one hydride would be expelled from the metal coordination sphere to an interstitial position. The topology of Li_4RhH_5 corresponds to such an expulsion of a coordinated hydride from RhH_5^{4-} to yield a square planar RhH_4^{3-} ion (i.e., $4Li^+$ $\{H^-\}$**[**RhH_2 $2H^-$**]** with two two 3c-4e$^-$ bonds and sd hybridization). Similar to Sr_2RhH_5, the neutron diffraction structures of Mg_2CoH_5[30] and Sr_2IrH_5[27] demonstrate monovacant O_h geometries of $[MH_5]^{n-}$ fragments consistent with monocationic Sr (see Table 1). In contrast, the structures of A_3PdH_5[20] and A_3PtH_5[19] (A ≡ K, Rb, or Cs) exhibit square planar metal hydride complexes with one "expelled" interstitial hydride per formula unit.

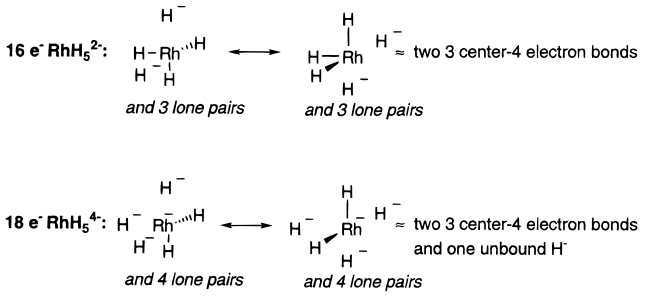

The isolated Sr_2RhH_5 molecule was modeled by using DFT computations and multiple minima were found, each corresponding to a different placement of the two Sr around a central RhH_5 unit as shown below in Table 2. The listed Sr charges are results of natural population analyses[56] and are consistent with Sr^{1+} ions.

When examined in detail, the crystallographic structure of Sr_2IrH_5 suggests resonance between the limiting Sr^+ and Sr^{2+} descriptions. For the Sr^{2+} description, a very long axial Rh−H distance corresponding to the weak interaction of the interstitial hydride and Rh is expected. In contrast, the Sr^+ description anticipates shorter axial than basal Ir−H bonds. The neutron

(56) Reed, A. E.; Weinstock, R. B.; Weinhold, F. *J. Chem. Phys.* **1985**, *83*, 735−746.

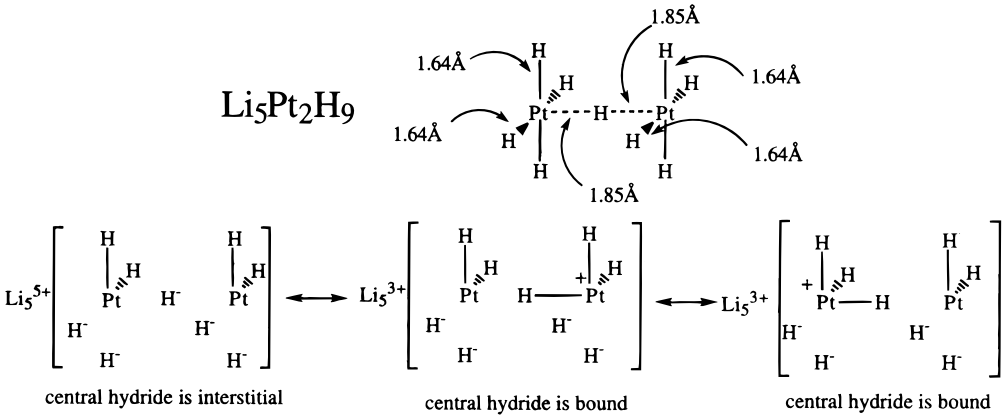

Figure 3. A graphic depiction of the crystallographic structure (top) of $Li_5Pt_2H_9$ and its decomposition into primary resonance structures (bottom).

diffraction structure of the low-temperature phase of Sr_2IrH_5[27] reveals a longer axial bond (1.82 Å axial vs 1.69 Å for basal hydrides). In contrast, the DFT models of molecular Sr_2RhH_5 exhibit longer basal bonds (ca. 1.69 Å) than axial bonds (ca. 1.56 Å). Hence, in the gas phase molecular Sr_2RhH_5 is well-described as having Sr^+ ions, but in the tightly packed, high dielectric medium of solid-state Sr_2IrH_5 the structure lies between the limiting extremes of Sr^+ (monovacant octahedral with short axial Ir−H bonds) and Sr^{2+} (square planar with an interstitial hydride) description.

A similar case is $Li_5Pt_2H_9$,[22] which has long axial Pt−H interactions (1.852(6) Å distant from each) between two nearly square planar PtH_4 groups. We describe this structure's *predominant* resonance configuration as five Li^+ monocations, two $16e^-$ square planar PtH_4^{2-} complexes, and an interstitial hydride. The rationalization for the bonding interaction between the Pt atoms and the "interstitial" hydride centers on significant contributions from other resonance structures (Figure 3). The lithium accepts sufficient electron density to make contributions from a configuration built from one $16e^-$ monovacant, octahedral $[PtH_5]^-$ complex, one square planar, $16e^-$ $[PtH_4]^{2-}$ complex, and Li_5^{3+} trication significant. The net result of resonance between these two localized resonance configurations is a semi-interstitial hydride between the Pt square planes. This structure lies between the extremes of the monovacant octahedron, as described for Sr_2IrH_5, and a square planar structure with a fully interstitial hydride, such as K_3PtH_5.[19]

Mg_3RuH_6 has been characterized in the solid state by neutron diffraction methods.[31] The structure consists of five hydrides coordinated to Ru and one interstitial hydride. The coordination geometry of the Ru is based on an octahedron with 5/6 overall occupancy (i.e., a monovacant octahedron) and was originally formulated[31] as an 18 electron $[RuH_5]^{5-}$. Our model allows us to formulate the compound as a 16 electron, $[RuH_5]^{3-}$ anion possessing two 3c-4e$^-$ bonds: $2Mg^+$ $1Mg^{2+}$ $\{H^-\}$**[**RuH_3^- $2H^-$**]**. This configuration leads to a formal charge of −1 at the Ru and sd^2 metal hybridization. As shown in Figure 1, occupation of five of six possible coordination sites will generate a monovacant octahedron.

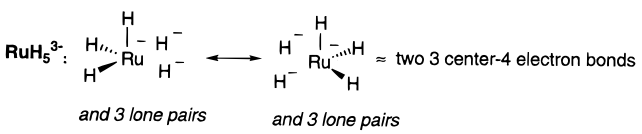

Adding a hydride to a 16 electron monovacant octahedron results in the familiar 18 electron octahedral complex. Examples of a compound with this shape in the solid state include A_3RhH_6 (A ≡ Na,[37] Li[36]), A_3IrH_6 (A ≡ Na,[37] Li[37]), and A_2PtH_6 (A ≡ Na,[40] K,[41] Rb,[42] Cs[42]) (Table 1). For ternary metal hydrides with alkaline earth elements, solid-state examples include A_2FeH_6 (A ≡ Mg,[32] Ca,[33] Sr,[33] Eu[33]), A_2OsH_6 (A ≡ Mg,[35] Ca,[33,34] Sr,[34] Ba[34]), and A_2RuH_6 (A ≡ Mg,[33,34] Ca,[26] Sr,[26] Ba[34]). Two formulations of these complexes are consistent with our postulated restrictions on formal charge and the order of delocalized bonding: (1) a 16 electron, dianionic metal hydride with a formal metal charge of 0 and monocationic alkaline earth elements and (2) an 18 electron, tetranionic metal hydride with formal metal charge of −1 and dicationic alkaline earth elements.

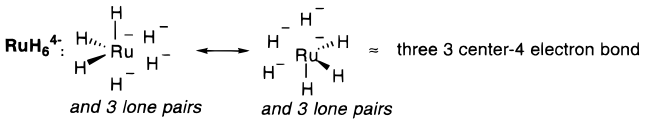

$BaMg_2MH_8$ (M ≡ Fe,[45] Ru,[46] Os[46]) compounds have been characterized by neutron diffraction and consist of $[MH_6]^{4-}$ octahedra and two interstitial hydrides per formula unit (Table 1). We formulate this compound as Ba^{2+} $2Mg^{2+}$ $\{2H^-\}$**[**MH_3^- $3H^-$**]**. A closely related example is $LiMg_4Os_2H_{13}$, which exhibits one interstitial hydride in the neutron diffraction structure.[48] We formulate this compound as Li^+ $4Mg^{2+}$ $\{H^-\}$ 2**[**OsH_3^- $3H^-$**]**.

Relationship to the Eighteen Electron Rule? Our VB description of transition metal bonding results in a set of rules for maximum electron count, but is different from the conventional $18e^-$ rule. In the VB description, each sd^n metal hybrid orbital commonly engages in a maximum of one 3c-4e$^-$ interaction. The solid-state ternary complexes with interstitial hydrides discussed above demonstrate that further expansion of the metal hydride coordination number is unfavorable. On the basis of the VB prescriptions described above, transition metal hydride complexes with various sd^n hybridizations are limited to the maximum electron counts listed in Table 3. Note that only complexes with sd^2 metal hybridization are strictly limited to a maximum 18 electron count according to our formalism.

The extension of these structures to sd^3 and higher metal hybridization implies the interesting possibility that complexes with an electron count of 20 or more may be isolable. In general, transition metal hydride complexes with more than 18 electrons will have substantial overall negative charges. In practice, destabilization due to high negative charges and loss of hydrides via elimination of H_2 may preclude their isolation. Even taken with minimal seriousness, these rules do suggest some formulations that could yield isolable complexes, especially at high pressures of H_2.

Table 3. Maximum Electron Counts Associated with Different Hybridizations

hybridization	maximum electron count	predicted shape of $[MH_x]^{n-}$ at max count	solid-state example
s	14	linear	$3K^+\{H^-\}[PdH^-\ H^-]$[11]
sd	16	square planar	$3K^+\{H^-\}[PtH_2\ 2H^-]$[19]
sd^2	18	octahedral	$Li^+2Mg^{2+}\{H^-\}[RuH_3^-\ 3H^-]$[44]
sd^3	20*	cubic	(unknown: $[IrH_8]^{3-}$?)
sd^4	22*	bicapped square prism?	(unknown: $[OsH_{10}]^{4-}$?)
sd^5	24*	icosahedral	(unknown: $[ReH_{12}]^{5-}$?)

It is also likely that ternary metal hydrides involving earlier transition metals can be made, although the cohesive energies of some of the pure metal phases may be so high that the ternary metal hydride phases, if formed, are metastable only.

Conclusions

In summary, we find that two rules based upon a localized VB viewpoint rationalize the complicated topologies and coordination geometries of solid-state ternary metal hydrides. The first rule stipulates that hypervalent metal hydrides with delocalizations greater than 3c-4e$^-$ bonding (such as 4c-6e$^-$ motifs) lose hydride ligands to interstitial positions. Application of this rule leads to a general framework for understanding the particular distribution of hydrides between complexation to the transition metal and occupation of interstitial positions. The second rule, which is a simple restatement of Pauling's electroneutrality rule, states that ternary metal hydrides favor transition metal formal charges of −1, 0, or 1. This restriction is in large part due to the similar electronegativities of transition metals and hydrogen;[5] these restrictions will not apply to all metal complexes (e.g., metal halides). Although ternary metal hydrides exhibit considerable delocalization of electron density and interesting band structures,[53] application of localized VB concepts lends considerable insight into some factors which control their structures. In this sense, ternary metal hydrides are seen to share some features with Zintl−Klemm compounds and their relatives in that (1) localized bonding models effectively describe the electronic structures of the anions,[57] (2) the extent of charge transfer from the alkaline earth metals may be one instead of two electrons,[58] and (3) hydrogen serves to stabilize these highly reduced systems with respect to forming intermetallic, or alloy, phases.[57] Extrapolation of these VB rules to their limit suggests that transition metal hydride complexes with greater than 18 electron counts may be feasible.

Computational Details

Molecular ternary hydrides were modeled with Gaussian 94[59] via density functional theory (DFT). Becke's 3-parameter functional[60] (B3) was used, with Lee, Yang, and Parr[61] (LYP) correlation energies. This method, DFT(B3LYP), has been shown to have accuracy comperable to sophisticated post-Hartree−Fock methods for transition metals and their monohydrides. The 6-311++G**[62−68] basis set was used for lighter elements through cobalt. For Sr, Ru, Rh, and Pd an effective core potential (ECP) was used to replace the first 28 electrons. The valence electrons on Sr were modeled with a (3111/3111/32)[69] contraction, while the transition metal basis sets used the (311111/22111/411)[70] contraction scheme. Pt was modeled with a Hay and Wadt ECP.[71] After geometry optimization, vibrational analysis was performed to ensure that true minima had been located. Natural bond order[55] (NBO) analysis and natural population analysis[56] (NPA) were used to analyze the resulting electron density.

Acknowledgment. This work was supported by a generous grant from the National Science Foundation. We gratefully acknowledge helpful discussions with Prof. Larry Dahl and Prof. Art Ellis.

Supporting Information Available: The results of ab initio computations are available (22 pages, print/PDF). See any current masthead page for ordering information and Web access instructions.

JA982746R

(57) Schäfer, H.; Eisenmann, B.; Müller, W. *Angew. Chem., Int. Ed. Engl.* **1973**, *12*, 694−712.
(58) Nesper, R. *Prog. Solid State Chem.* **1990**, *20*, 1−45.
(59) Frisch, M. J.; Trucks, G. W.; Schlegel, H. B.; Gill, P. M. W.; Johnson, B. G.; Robb, M. A.; Cheeseman, J. R.; Kieth, T.; Petersson, G. A.; Montgomery, J. A.; Raghavachari, K.; Al-Laham, M. A.; Zakrzewski, V. G.; Ortiz, J. V.; Foresman, J. B.; Cioslowski, J.; Stefanov, B. B.; Nanayakkara, A.; Challacombe, M.; Peng, C. Y.; Ayala, P. Y.; Chen, W.; Wong, M. W.; Andres, J. L.; Replogle, E. S.; Gomperts, R.; Martin, R. L.; Fox, D. J.; Binkley, J. S.; Defrees, D. J.; Baker, J.; Stewart, J. P.; Head-Gordon, M.; Gonzalez, C.; Pople, J. A.; Gaussian, Inc.: Pittsburgh, PA, 1995.
(60) Becke, A. D. *Phys. Rev. A* **1988**, *38*, 3098.
(61) Lee, C.; Yang, W.; Parr, R. G. *Phys. Rev. B* **1988**, *37*, 785−789.
(62) McLean, A. D.; Chandler, G. S. *J. Chem. Phys.* **1980**, *72*, 5639.
(63) Krishnan, R.; Binkley, J. S.; Seeger, R.; Pople, J. A. *J. Chem. Phys.* **1980**, *72*, 650.
(64) Wachters, A. J. H. *J. Chem. Phys.* **1970**, *52*, 1033.
(65) Hay, P. J. *J. Chem. Phys.* **1977**, *66*, 4377.
(66) Raghavachari, K.; Trucks, G. W. *J. Chem. Phys.* **1989**, *91*, 1062.
(67) Clark, T.; Chandrasekhar, J.; Spitznagel, G. W.; Shleyer, P. v. R. *J. Comput. Chem.* **1983**, *4*, 294.
(68) Frisch, M. J.; Pople, J. A.; Binkley, J. S. *J. Chem. Phys.* **1984**, *80*, 3265−3269.
(69) Kaupp, M.; Schleyer, P. v. R.; Stoll, H.; Preuss, H. *J. Chem. Phys.* **1991**, *94*, 1360.
(70) Andrae, D.; Haeussermann, U.; Dolg, M.; Stoll, H.; Preuss, H. *Theor. Chim. Acta* **1990**, *77*, 123.
(71) Hay, P. J.; Wadt, W. R. *J. Chem. Phys.* **1985**, *82*, 271−284.